Palaeontologia Electronica
http://palaeo-electronica.org

THE IMPACT OF ASYMMETRIES IN THE ELEMENTS OF THE PHRAGMOCONE OF EARLY JURASSIC AMMONITES

Louise M. Longridge, Paul L. Smith, George Rawlings, and Voytek Klaptocz

ABSTRACT

In many Early Jurassic ammonites including *Badouxia columbiae* (Frebold 1967), the siphuncle is offset from the midline of the venter. In these cases, the septal suture line is expanded on the opposite side of the shell, suggesting an expansion of the septum on the non-siphuncle side. We use three computer models of *B. columbiae* to examine the hydrostatic implications of these asymmetries with respect to the presence of a possible weight-balancing mechanism. The first model is limited to the internal elements of a single chamber of the phragmocone including the siphuncle and septum. Cameral sheets are also considered mathematically as an optional component. The model indicates a counterbalance mechanism may have been present as the mass of the offset siphuncle (and optional cameral sheets) is at least partially corrected by the increased mass of the septum on the opposite side. In order to examine the affect of these asymmetries on the entire ammonite, two models representing complete ammonites at large and small shell diameters were constructed. In both cases, results show that the siphuncle and septal asymmetries within the phragmocone are very small with respect to the mass of the animal, and the effect of the offset components is insignificant. The asymmetric position of the siphuncle simply forced expansion of the septal suture line and septal folds on the non-siphuncle side of the shell but no significant counterbalance was in effect.

Louise M. Longridge. Earth and Ocean Sciences, University of British Columbia, 6339 Stores Road, Vancouver, British Columbia, V6T 1Z4, Canada. llongridge@eos.ubc.ca
Paul L. Smith. Earth and Ocean Sciences, University of British Columbia, 6339 Stores Road, Vancouver, British Columbia, V6T 1Z4, Canada. psmith@eos.ubc.ca
George Rawlings. Mechanical Engineering, University of British Columbia, 2054-6250 Applied Science Lane, Vancouver, British Columbia, V6T 1Z4, Canada. rawlings@mech.ubc.ca
Voytek Klaptocz. Mechanical Engineering, University of British Columbia, 2054-6250 Applied Science Lane, Vancouver, British Columbia, V6T 1Z4, Canada. voytek@mech.ubc.ca

KEY WORDS: ammonite; asymmetric siphuncle; septa; computer models; Early Jurassic

PE Article Number: 12.1.1A

Submission: 31 March 2008. Acceptance: 29 December 2008

Longridge, Louise M., Smith, Paul L., Rawlings, George, and Klaptocz, Voytek 2009. The Impact of Asymmetries in the Elements of the Phragmocone of Early Jurassic Ammonites. *Palaeontologia Electronica* Vol. 12, Issue 1; 1A: 15p;
http://palaeo-electronica.org/2009_1/160/index.html

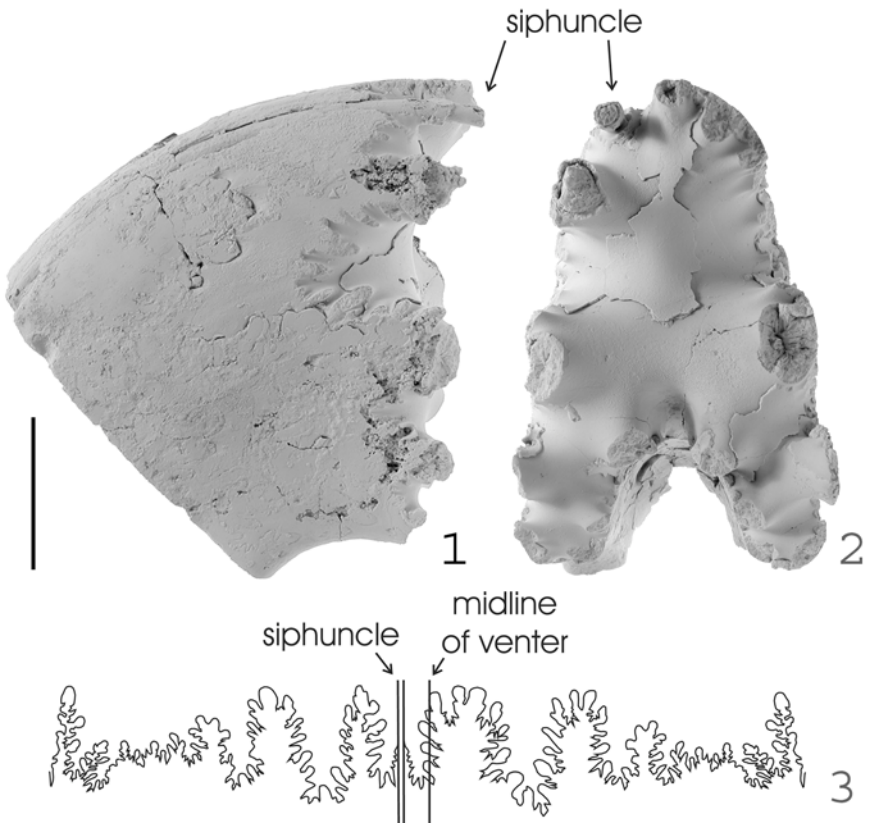

FIGURE 1. Scanned fragment of *Badouxia columbiae* (Frebold), (1) Lateral view, (2) Frontal view, scale bar = 2 cm. (3) Septal suture line from *B*. *columbiae* used in creating model 1. Scale equals 4 cm.

INTRODUCTION

Counterbalance mechanisms were prevalent in straight-shelled Paleozoic cephalopods such as Actinoceratoids and Endoceratoids (Westermann 1998). These groups used calcium carbonate to weight their distal ends in order to orientate their soft bodies away from the dangers of the substrate while improving their hydrodynamic efficiency when moving across the ocean floor. Once these groups became extinct in the Middle to Late Paleozoic, counterbalance mechanisms became obsolete. However, some Jurassic ammonites have asymmetries in the elements of their phragmocone, which raises the question as to whether a counterbalance mechanism was in effect, allowing the animal to remain upright in the water column.

Following the end-Triassic mass extinction, *Psiloceras* formed the root stock for the Jurassic and Cretaceous ammonite radiation (e.g., Guex 2006). In a typical planispirally coiled ammonite, the siphuncle usually ran centrally along the venter of the shell within the plane of bilateral symmetry. However, in many species of Jurassic ammonites, it has long been recognized that the siphuncle can be considerably offset to one side (e.g., Canavari 1882; Swinnerton and Trueman 1917; Spath 1919; Hölder 1956; Hengsbach 1986a, b; Guex 2001). Although some researchers believed it was of no biological importance (e.g., Diener 1912), several biological explanations have been proposed. Spath (1919, p. 116, 118 and references therein) suggested it may be one line of evidence of an attempt to change a bilaterally symmetric swimmer into a crawling benthic organism. In the case of flat ventered shells, Swinnerton and Trueman (1917) hypothesized that asymmetry allowed the siphuncle to take up a stable position along the ventrolateral shoulder. Hengsbach (1979, 1986a, b, 1991, 1996) proposed that an asymmetric siphuncle may be due to the presence of parasites in early ontogeny that caused displacement of the root of the siphuncle. Recent work has highlighted the role of external stress in increasing the rate of gene mutation and recombination as well as in the initiation of asymmetries (Hoffman and Parsons 1991). It seems possible that environmental stress in the earliest Jurassic may have generated asymmetry of the siphuncle in the ammonite root stock (Guex 2001). Subsequently, this character persisted inter-

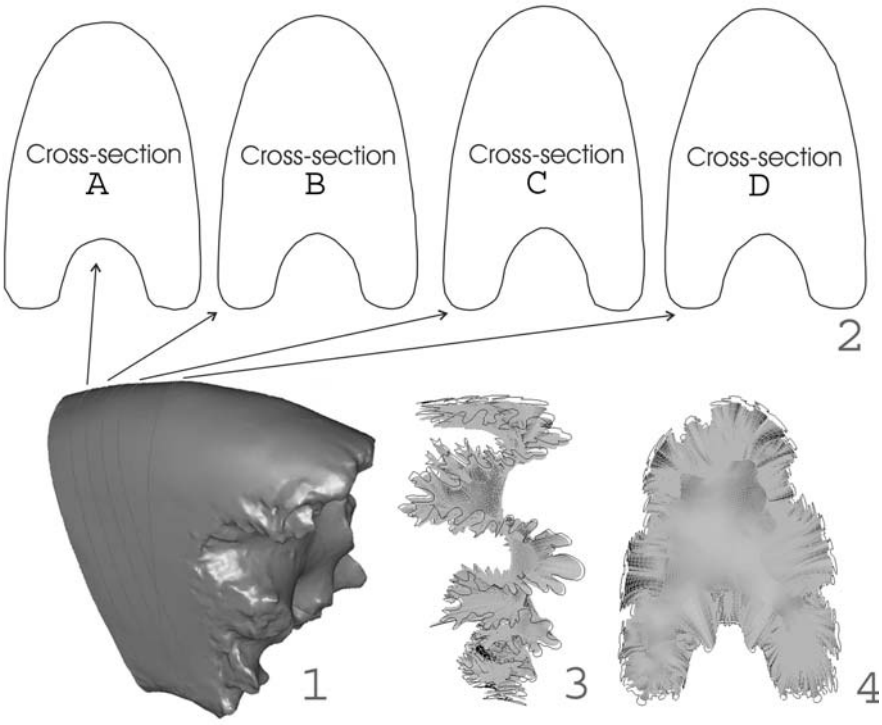

FIGURE 2. (1) Computer model of scanned fragment shown in Figure 1. (2) Cross-sections taken from model using Rhinoceros. Model of septum with superimposed suture line, (3) Lateral view, (4) Frontal view.

mittently within the Jurassic part of the ammonoid evolutionary radiation.

The attitude of an ammonite in the water column is a product of the location of its centres of buoyancy and mass (Trueman 1941). While the position of the centre of buoyancy is unaffected by changes within the conch, the centre of mass is dependent on the volume, density and position of individual components. Ammonites with offset siphuncles have expansion in the elements of the septal suture line on the non-siphuncle side (Figure 1.3). It seems possible that the displaced mass caused by the offset siphuncle may have been balanced by the mass of expanded septa on the opposite side of the conch, permitting the animal to stay vertical in the water. We use computer models of the earliest Sinemurian ammonite, *Badouxia columbiae* (Frebold 1967) to examine the hydrostatic implications of these siphuncular and septal asymmetries.

METHODS

We developed two types of computer model. The first (model 1), of a single septum and one chamber length of siphuncle, was used to examine the effects of asymmetry within a single chamber of the ammonite's phragmocone. The second type of model is of a complete ammonite, which allowed us to examine the potential effects of phragmocone asymmetries on the entire ammonite animal. In this case, two models of different shell diameter were constructed (models 2 and 3) permitting analysis of the impact of phragmocone asymmetries at different growth stages. All measurements were taken from specimens of *B. columbiae*. Abbreviations and measurements follow Smith (1986) and include maximum shell diameter (DMAX) and whorl height (WH). Details of model construction are given below.

Model 1: Components within a Single Phragmocone Chamber

Scanned Fragment. Model 1 was based on an ammonite whorl fragment that had a well exposed septal face (GSC 131683, Figure 1.1-1.2). A three-dimensional scan of this fragment was created at Memorial University in St. John's, Newfoundland, using a FARO platinum arm with laser line probe. Details of the scanner can be found at http://www.faro.com/content.aspx?ct=uk&content=pro&item=1. The scanned data were imported into the three-dimensional CAD modeling program and surface triangulation software, Geomagic. In this program, the scanned model was edited to create a three-dimensional outline of the fossil (Figure 2.1). Digital processing error and surface imperfec-

tions such as minor surface cracks caused by weathering were smoothed out manually. The fossil outline was exported to the surface modeling and engineering analysis software Rhinoceros, which is capable of calculating a range of geometric properties including volumes and surface areas of various geometries. Details of the program can be found at http://www.rhino3d.com. Several different cross-sections were taken to check for symmetry about the centre line (Figure 2.2). The whorl shape was found to be symmetric within reasonable error (Table 1).

TABLE 1. Measurements from the cross-sections in Figure 2.2 divided down the median line.

Cross-section number	Left half (mm)	Total (mm)	Percentage
A	19.12	38.09	50.20
B	19.44	38.71	50.22
C	19.69	39.09	50.37
D	19.45	39.00	49.87

Single Septum. Using Geomagic, the septal face was lifted off the fossil scan. Due to erosion, the ventral tips of the saddles were missing from the scan. Thus, the geometry extending from approximately the outer third of the septal face to the suture line had to be reconstructed. The outermost edges of the scanned septal face were cropped off, and the innermost two-thirds of the septal face were imported into Rhinoceros. The septal suture line directly preceding the scanned septal face (Figure 1.1) was used in combination with parts of a suture line from another specimen where necessary, to create a complete suture line (Figure 1.3). This two-dimensional suture line was projected onto the scanned shell and scaled to ensure the peaks and saddles correlated with the septal face and identifiable landmarks on the scan. Approximately 1500 lines tangent to the edge of the septal face were hand-drawn, joining the edge of the septal face to the suture line. Finally, a surface was lofted through these lines resulting in a complete septal face, composed of the scanned central part with modeled edges extending out to the superimposed suture line (Figure 2.3-2.4).

In order to calculate their thickness, thin sections were cut perpendicular to septa (Figure 3.1) at three different shell diameters. It is well recognized that ammonite septa thin from the centre towards the margins of the shell (Westermann 1971). This was accounted for by measuring the thickness at the middle of each septa as well as the thickness of the very outside edge. These thicknesses were then plotted against whorl height, and the average of the two values was used to represent the thickness of the septa at a given whorl height (Figure 4.1).

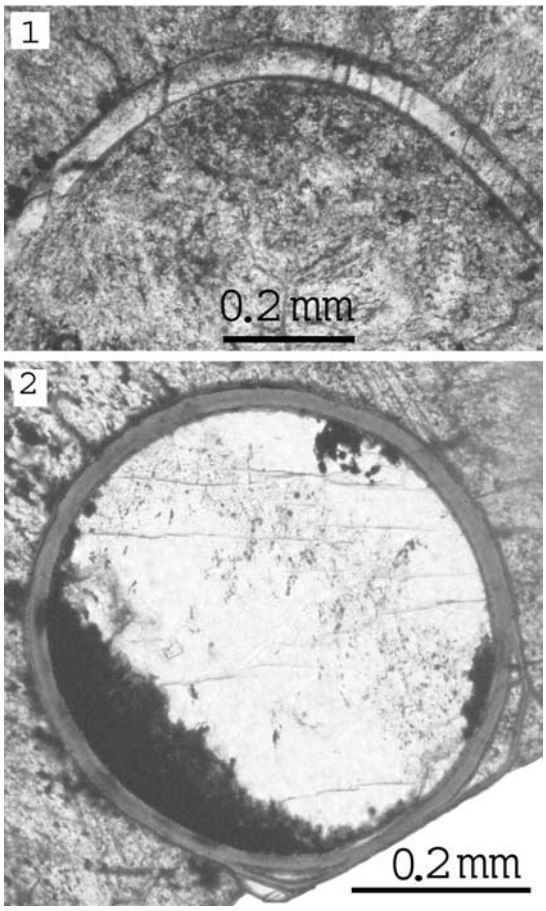

FIGURE 3. (1) Thin section showing middle portion of septum cut perpendicular to face. (2) Thin section cut perpendicular to siphuncle.

The area of the septal face was obtained using a built-in function within Rhinoceros. By multiplying the septal face surface area from the model by the thickness from the graph, a volume was established for the ammonite septum (Table 2). It is well documented that ammonite septa were composed principally of aragonite (e.g., Kulicki 1996), which has usually reverted to calcite during diagenesis. Analysis of the measured septa using x-ray diffraction confirmed they had altered to calcite. As volume increases when aragonite is altered to calcite (e.g., Liu and Yund 1993), the volumes taken

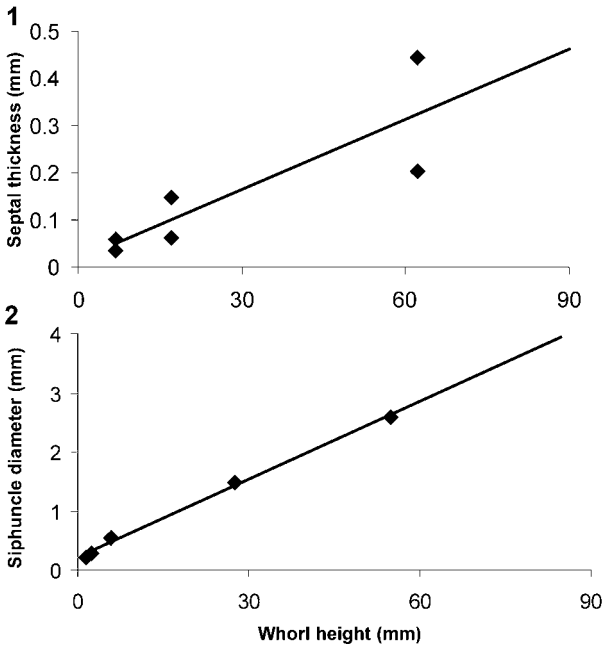

FIGURE 4. Plot of measurements of model components, (1) Septal thickness versus whorl height, (2) Siphuncle diameter versus whorl height.

from the model were reduced by 7.6 % before being included in the calculations. This percentage was calculated using the following equations:

If density = mass/volume and mass is constant then

Equation (1): volume calcite (A) = 1 g/2.71 g/cm^3 = 0.369 cm^3

Equation (2): volume aragonite (B) = 1 g/2.93 g/cm^3 = 0.341 cm^3

Equation (3): volume difference = A - B = 0.028 cm^3

Equation (4): total volume change = 0.028 cm^3/ 0.369 cm^3 x 100 % = 7.6 %

The density used for the septa was the same as for the shell (2.67 g/cm^3, Hewitt and Westermann 1996) and was used in combination with the adjusted volume to produce a mass of about 4.12 g for the modeled septum (Table 2).

Single Chamber Length of Siphuncle. The length of siphuncle within a single chamber was measured directly from the scanned fragment (25.7 degrees, 33.8 mm, Figure 1.1). In order to calculate the diameter of the siphuncle, five polished thin sections were cut perpendicular to the siphuncle at different whorl heights (Figure 3.2). In each case, the siphuncle diameter was then measured and plotted against whorl height (Figure 4.2). A best fit line was applied to this graph and measurements were taken from this line to assign the siphuncle diameter to the model. A recent study of Cretaceous phylloceratids found that as ammonites grew, new siphuncular tissue was added in front of the last formed septum (Tanabe et al. 2005). Based on this finding, the centre of the chamber length of the siphuncle in our model was added such that it intersected the septum. Using the model, the volume was determined by capping each end of the siphuncle and using a built-in function in Rhinoceros (Table 2). The siphuncular tube consists of conchiolin membranes and is very thin (Westermann 1971; Tanabe et al. 2005). It is primarily filled with blood vessels and surrounding epithelium (Tanabe et al. 2000). For this reason, the density of the siphuncle was taken as 1.055 g/cm^3, the same as the density of the soft body of *Nautilus* (Saunders and Shapiro 1986). The product of density times volume produced a mass of about 0.24 g for the siphuncle on the model (Table 2).

Cameral Sheets. Sheets of organic material have been discovered in the chambers of Triassic, Jurassic and Cretaceous ammonites (Grandjean 1910; Weitschat and Bandel 1991; Westermann 1992; and references therein) and may have been present in *B. columbiae*. Thus, cameral sheets are included mathematically in model 1 as a separate, optional component. Cameral sheets are broadly divided into three groups: horizontal sheets, siphuncular sheets and transverse sheets

TABLE 2. Volumes, densities, masses, offset distances and moments of force for the morphological components of model 1.

Morphological component	Volume (mm^3)	Density (g/cm^3)	Mass (g)	Offset distance (mm)	Moment of force (g*mm)
siphuncle	226.65	1.055	0.24	5.87	1.41
septum	1542.70	2.670	4.12	-1.01	-4.16
cameral sheets	3455.45	1.055	3.65	2.78	10.15

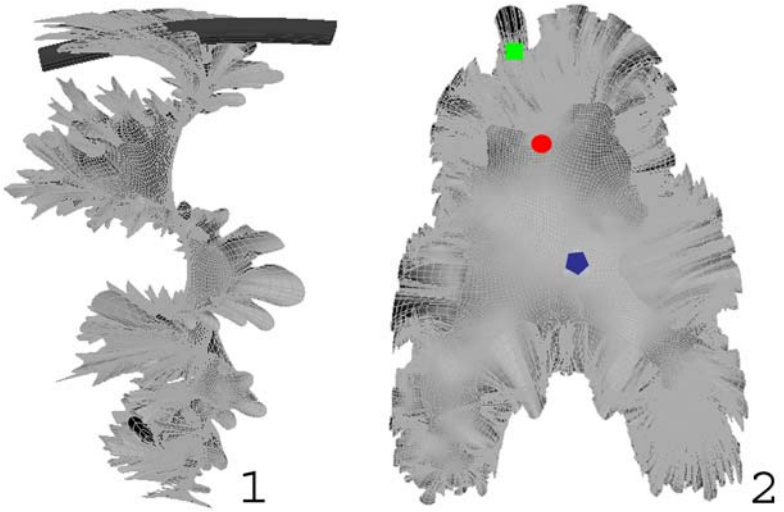

FIGURE 5. Completed model of single septum including one chamber length of siphuncle, (1) Lateral view, (2) Frontal view. Blue pentagon represents centroid of septum, red circle represents centroid of cameral sheets, green square represents centroid of siphuncle.

(Weitschat and Bandel 1991). Horizontal sheets are not included here as they are probably limited to Triassic ammonites with nearly spherical conchs (Westermann 1992). Siphuncular sheets are usually short and straight in Jurassic ammonites and probably functioned to attach the siphuncle to the inner shell wall whereas transverse sheets include all sheets that are subparallel to the septa including some that are suspended from the siphuncular tube (Weitschat and Bandel 1991). As both the latter two types of cameral sheets are associated with the siphuncle, in cases where the siphuncle is offset to one side, their mass would also have been displaced. Cameral sheets probably occupied a total of about 14 % of cameral space (Hewitt and Westermann 1996; Kröger 2002). In model 1, 9.5 % of cameral space is considered to be occupied by cameral sheets (as horizontal sheets were not present). The siphuncular sheets would have been completely offset as they surrounded the siphuncle (3 % of chamber volume was allocated for these). In addition, a portion of the transverse sheets would also have been offset as some of these are suspended from the siphuncle (1.5 % of chamber volume was allocated for these). Thus, in the model, 4.5 % of the volume of the chambers was considered to be taken up by cameral sheets that were offset whereas the remaining 5 % of chamber volume was considered to be occupied by cameral sheets that were considered central. Total chamber volume was determined directly from the model using the built-in function in Rhinoceros (Table 2). As cameral sheets are believed to have been organic in composition (e.g., Erben and Reid 1971; Weitschat and Bandel 1991 and references therein) and saturated with cameral liquid (Kröger 2002), the density of the cameral sheets is considered to be 1.055 g/cm^3, the same as the soft tissue of *Nautilus* (Saunders and Shapiro 1986). The product of density times 9.5 % of total modeled chamber volume produces a mass of about 3.65 g for the cameral sheets (Table 2).

Complete Model. Except for the optional cameral sheets that are only included in calculations, the complete model is shown in Figure 5. The position of the centroids of the septum and siphuncle were calculated from the model using a built-in function within Rhinoceros (Figure 5.2). In this paper, the centroid of a component is taken as its geometric centre. In the case of the models discussed herein, all the components are considered to have had a uniform density. Thus, the centroid coincides with the centre of mass, and the two terms are used interchangeably throughout the paper. For the cameral sheets, the position of the centroid is taken as the average offset distance of all the sheets weighted according to the percentages discussed above (Figure 5.2). The distances of offset from the centre line are indicated in Table 2.

Model 2: Entire Ammonite Animal at 300 mm Shell Diameter

To investigate how these asymmetries affected the entire ammonite animal, a three-dimensional model of a specimen of large shell diameter was constructed (model 2, DMAX = 300 mm). Required data included whorl dimensions as well as septal face surface areas, thickness and

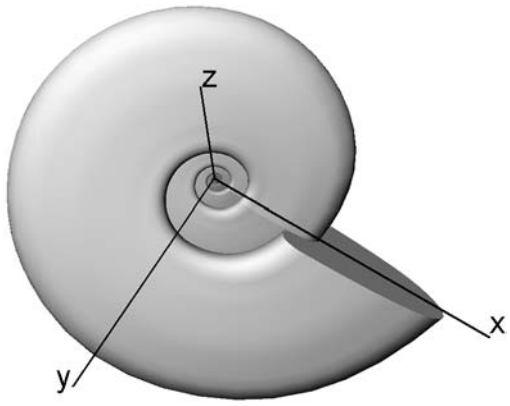

FIGURE 6. Direction notation for models 2 and 3.

number of septal faces, siphuncle diameter, shell thickness and body chamber length. Procedures used to calculate each of these components are addressed below. Direction notations for the model are indicated in Figure 6.

Whorl Dimensions. The inner and intermediate portion of the model was created using measurements taken from the specimen of *B*. *columbiae* shown in Figure 7.1 (GSC 127377, DMAX = 197 mm). In addition, a fragment of the outer whorl of a large, incomplete specimen (Figure 7.2, GSC 131683, WH = 132.6 mm) was used to provide information for the model at large shell diameter. This whorl fragment is from the same ammonite as the scanned fragment used as the basis for model 1 but is about 360 degrees larger in size. Measurements of the distance of the generating curve from the coiling axis (Raup 1967), whorl height and whorl width were measured at a number of positions and used to provide the model dimensions. These measurements were plotted as a function of angle. The 0 degree position in the model was set as the start of the shell at maximum shell diameter

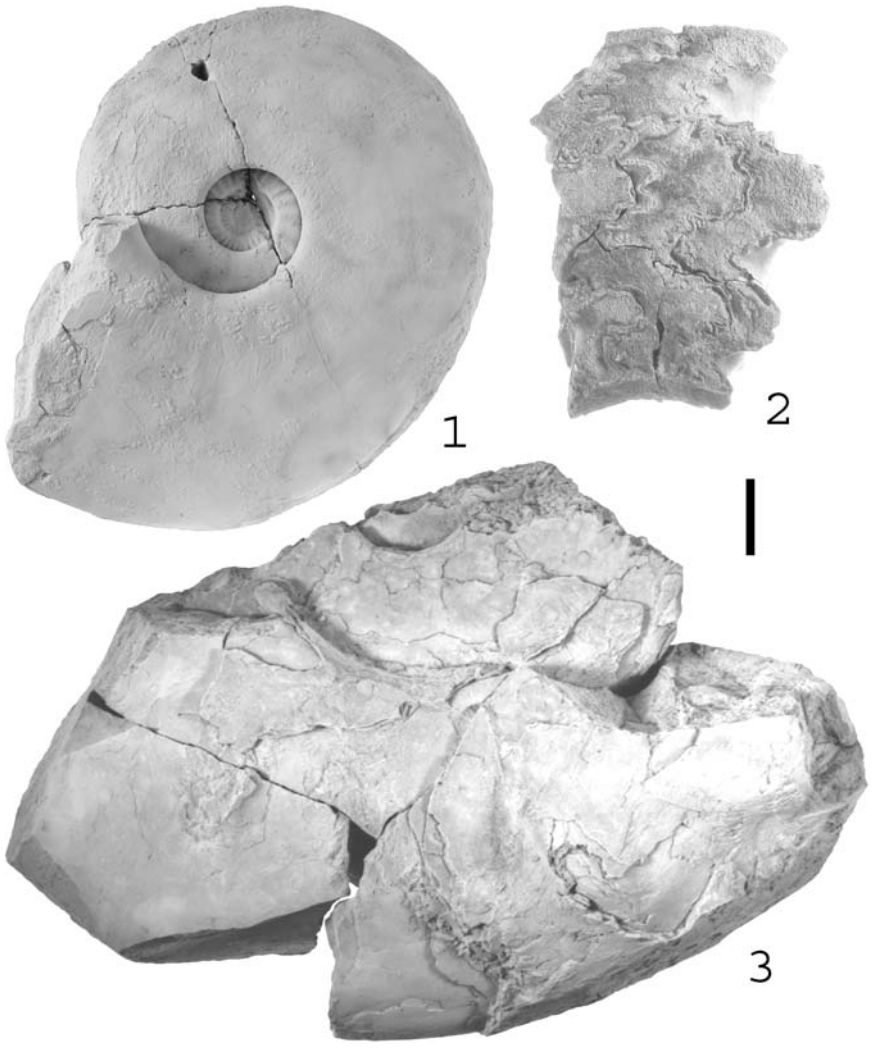

FIGURE 7. Specimens and fragments of *Badouxia columbiae* (Frebold 1967), (1) Specimen used for measurements of inner and intermediate whorls of ammonite model 2 and all of model 3. Scale equals 2.5 cm. (2) Fragment of large whorl used for measurements of outer whorl of ammonite model 2 and body chamber length. Scale equals 2.5 cm. (3) Incomplete specimen where outermost whorl is body chamber. Scale equals 4 cm.

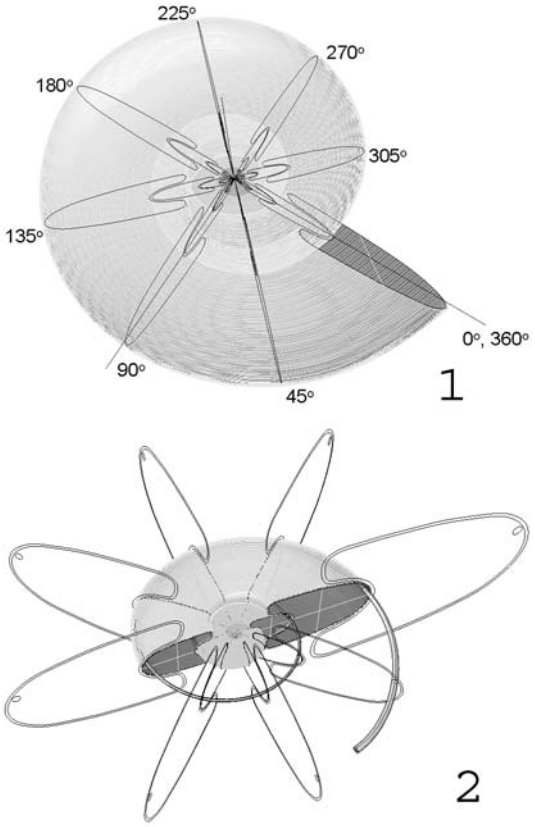

FIGURE 8. (1) Angle convention for model assembly, (2) Model assembly.

(DMAX = 300 mm), and the outermost 360 degrees of rotation is termed the first whorl. In other words, the angular position increases proceeding towards the umbilicus (Figure 8.1). The original cross-section from the scan was scaled in width and height to match the curve fit through the measured values at 45 degree increments (Figure 8.2). A total of seven whorls for an angle index up to 2520 degrees were drawn; however, given the very small size of the innermost whorl (DMAX = 1.2 mm), only the first six whorls (up to 2160 degrees) were modeled in detail and used for analysis.

Septal Face Surface Areas. Model 1 provided a septal face surface area of 5098.52 mm^3 for a whorl height of 62.3 mm. In order to examine how septal face surface areas changed through ontogeny, two more septal face surface areas were needed. Each of these was calculated using the following equations:

Equation (1): If unknown septal face surface area = A, unknown whorl cross-section surface area = B, septal surface area of scanned face = C and scanned whorl cross-section surface area = D then A = (C x B)/D.

However, A needs to be adjusted to take into account the simplification of the suture line as shell diameter decreases using a simplification factor (equations 2-4).

Equation (2): If suture line length of unknown septal face = E and whorl perimeter length of unknown face = F then E/F = G.

Equation (3): If suture line length of scanned septal face = H and whorl perimeter length of scanned septal face = I then H/I = J.

In order to calculate the suture line length for equations 2 and 3, the suture lines were drawn, flattened and then measured.

Equation (4): The simplification factor is G/J = K.

Equation (5): Therefore, the actual unknown septal face surface area (L) = A x K.

The two calculated surface areas as well as the septal face surface area from the scanned specimen were then plotted against whorl height (Figure 9.1). A curve was fitted through the three values to allow for a septal surface area estimate for each septum.

Septal Thickness and Number. The best fit line for the graph of septal thickness versus whorl height described for model 1 was used to assign a thickness to each septum (Figure 4.1). The number of septa per 360 degrees was counted in a specimen at several ontogenetic stages and then plotted against the whorl height measured at the large end of each revolution (Figure 9.2). For the purposes of model construction, the average number of septa per whorl was taken as 14, and they were placed every 25.7 degrees behind the septum at the back of the body chamber.

Siphuncle Diameter. As in model 1, the best fit line for the graph of siphuncle diameter plotted against whorl height was used to assign diameters to the siphuncle in the model (Figure 4.2).

Although the specimen used to make the shell measurements is quite small (DMAX = 74 mm) relative to the model, Westermann (1971) showed that shell wall thickness in the Ammonitina is approximately isometric or even positively allometric with shell diameter. Thus, we consider the plot to be reasonably accurate for extrapolation of data at larger shell diameters.

Shell Thickness. Only one specimen of *B. columbiae* had an intact shell that was suitable for thickness measurements (Figure 10, GSC 127319). Following the method used by Kröger (2002), measurements were taken at six different whorl heights. In each case, fragments of shell were

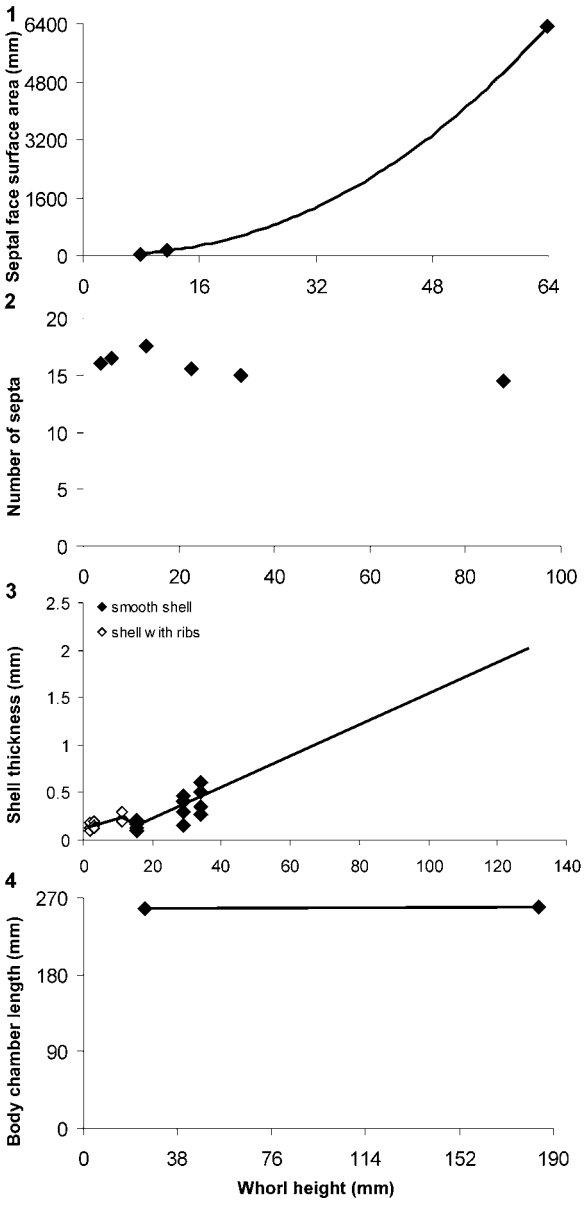

FIGURE 9. Plot of measurements of model components. (1) Septal face surface area versus whorl height, (2) Number of septa versus whorl height, (3) Shell thickness versus whorl height, (4) Body chamber length versus whorl height.

removed by hand from five different areas of the whorl; specifically, the umbilical shoulder, lower flank, midflank, upper flank and venter. Each fragment was measured using microcalipers. The average of the five measurements was calculated, and the average thickness value was plotted against whorl height (Figure 9.3). A curve was fitted through the measured values to allow for a shell thickness estimate at each 45 degree increment. There was a slight increase in shell thickness on the innermost whorls due to the presence of ribs in the shell (Figure 9.3).

Cameral Sheets. Similar to model 1 described above, cameral sheets were considered as an optional component.

Body Chamber Length. Body chamber length was measured at two different shell diameters. In the first case, a body chamber length of 258 degrees was measured on a small specimen (Figure 9.4, GSC 131684, WH = 25 mm). In the second case, the body chamber length had to be estimated because complete specimens of *B. columbiae* at large shell diameters are unknown. The large fragment used to create the model has approximating septa and is the final portion of a mature phragmocone (Figure 7.2, GSC 131683, WH = 132.6 mm). This fragment was used in combination with a second incomplete specimen where the final portion of phragmocone is missing but the body chamber is present (Figure 7.3, GSC 127056). By inferring the position of the septate fragment, a body chamber length of about 259 degrees was obtained. Because both the observed and calculated body chamber lengths were very similar, a length of 259 degrees was adopted for the model.

Model Assembly. Once the dimensions of all the components were obtained, the model was assembled using Rhinoceros. Whorls (containing shell and siphuncle outline) of similar absolute angle (i.e., 0, 360, 720, etc. degrees) were fitted together and rotated into position. Surfaces were then lofted onto the shell, body and siphuncle outlines, and ends were put onto the lofted surfaces to make volume calculations possible (Figure 8.2). Finally, the model was divided into whorl or half-whorl portions to facilitate easy removal for work on smaller specimens.

Component Masses and Positions. Volumes were obtained from the model for the shell, siphuncle and body chamber using functions built into the software (Table 3). The total volume of the septa was calculated as the product of the septal face surface areas times thicknesses. As discussed for the septum in model 1, the volumes of the septa and shell were reduced by 7.6 % before being included in the model to account for the change of volume caused by aragonite inverting to calcite (Table 3). To obtain the volume of cameral sheets, total chamber volume was calculated by subtracting the volume of the septa from the total volume of the interior of the phragmocone obtained from the model. As in model 1, the volume of cameral

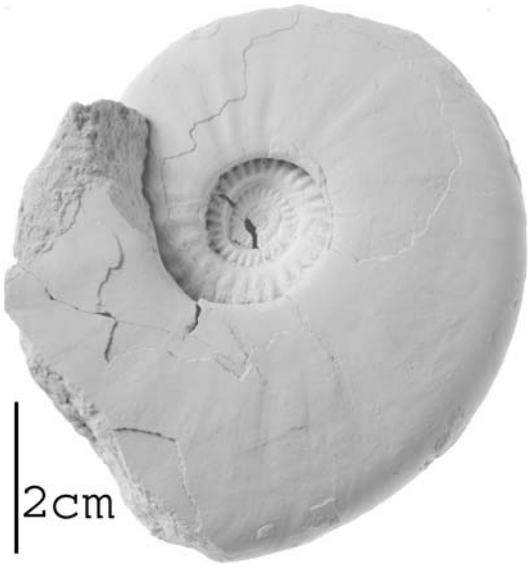

FIGURE 10. Specimen of *Badouxia columbiae* (Frebold 1967) used for shell thickness measurements.

sheets was included at 4.5 % offset with a total of 9.5 % of chamber volume being filled. Similar to model 1, the density used for the septa and shell was 2.67 g/cm^3 (Hewitt and Westermann 1996) whereas the density used for the siphuncle, cameral sheets and body chamber was 1.055 g/cm^3 (Saunders and Shapiro 1986). Density multiplied by volume provided the mass of each component (Table 3). The position of the centroid of each individual component in the X, Y and Z plane with respect to the origin is given in Table 3 (Figure 11). The origin (X, Y, Z = 0, 0, 0) is the very centre of the model. In the innermost whorl, the position of the siphuncle is variable but by the next whorl the position of the siphuncle is reasonably stable, and the suture line is consistently expanded on the non-siphuncle side and reduced on the siphuncle side. Thus, we considered the offset distances of the siphuncle, septa and cameral sheets to be the same as in model 1 (Table 2). Finally, the data for each component was combined, and centres of buoyancy and mass were calculated for the entire ammonite animal. The centres of mass (total X, Y and Z coordinates in Table 4) and buoyancy (displacement in Table 4) are shown in Figure 12. The final X, Y and Z coordinates are calculated from the total weighted coordinate for each axis divided by the total mass of the animal.

Model 3: Entire Ammonite Animal at 54 mm Maximum Shell Diameter

To investigate how these asymmetries affected the entire ammonite animal at different growth stages, a three-dimensional model of a complete, small ammonite animal was also created (model 3, DMAX = 54 mm). Model 3 was constructed by removing the outer two whorls from model 2 and altering the position of the body chamber. The volumes were calculated using the same methods described above for model 2, and the densities used for each component are the same as in model 2 (Table 5). Volumes, masses and relative positions of the centroids of each component in the X, Y and Z plane are given in Table 5 whereas the positions of the centres of buoyancy (displacement) and mass (final X, Y and Z coordinates) are provided in Table 6. Once again, cameral sheets are kept optional.

RESULTS AND DISCUSSION

Although living ammonoids are considered to have been only very slightly negatively buoyant (Westermann 1996 and references therein), an accurate model of an immature ammonite should

TABLE 3. Volumes, densities, masses and positions of individual X, Y and Z coordinates for each morphological component of model 2.

Morphological component	Volume (mm^3)	Density (g/cm^3)	Mass (g)	X coordinate (mm)	Y coordinate (mm)	Z coordinate (mm)
siphuncle	1978.88	1.055	2.09	31.01	-7.14	5.36
septa	14826.40	2.670	39.59	20.68	-10.52	-0.96
cameral sheets	31957.96	1.055	33.72	26.11	-6.25	2.54
shell	219446.64	2.670	585.92	17.90	37.87	0
body chamber	2011601.90	1.055	2122.24	17.43	47.80	0

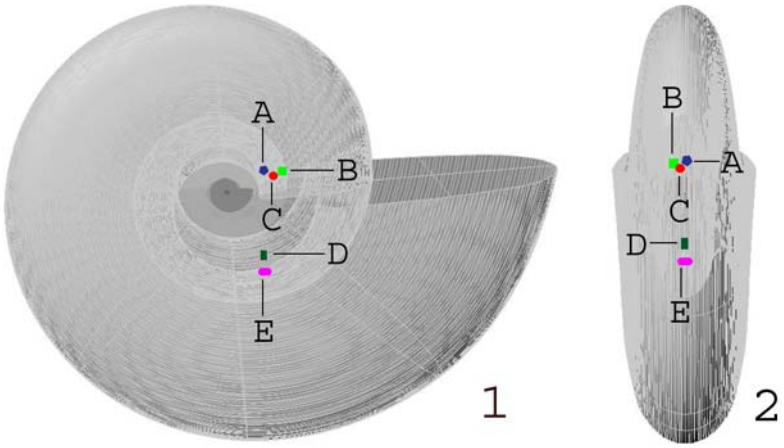

FIGURE 11. Model showing centres of mass for each element of animal, (1) Lateral view, (2) Ventral view. A, Septa; B, Siphuncle; C, Cameral membranes; D, Shell; E, Body chamber.

TABLE 4. Masses and positions of total X, Y and Z coordinates for model 2 (cameral sheets optional). Total displacement and position of centre of buoyancy is also indicated.

Complete model	Mass (g)	X coordinate (mm)	Y coordinate (mm)	Z coordinate (mm)
without cameral membranes	2749.84	17.52	44.80	-0.01
with cameral membranes	2783.56	17.63	44.18	0.02
displacement	2722.02	17.61	37.30	0

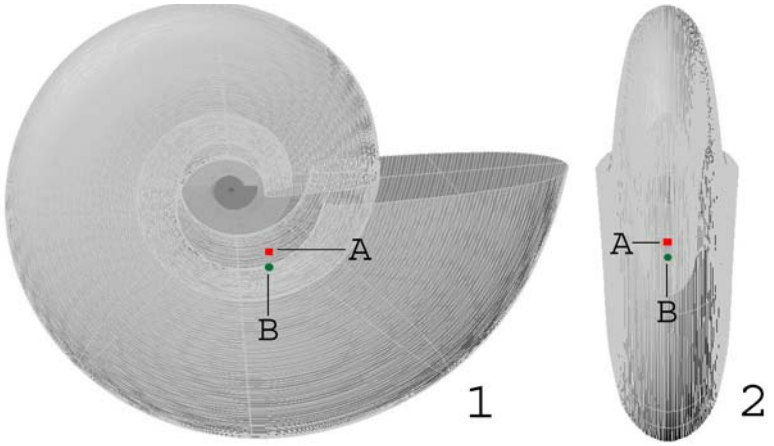

FIGURE 12. Model showing centres of buoyancy and mass for animal, (1) Lateral view, (2) Ventral view. A, Centre of buoyancy; B, Centre of mass.

TABLE 5. Volumes, densities, masses and positions of individual X, Y and Z coordinates for each morphological component in model 3.

Morphological component	Volume (mm^3)	Density (g/cm^3)	Mass (g)	X coordinate (mm)	Y coordinate (mm)	Z coordinate (mm)
siphuncle	22.14	1.055	0.02	4.36	-1.00	0.96
septa	62.88	2.670	0.17	3.34	-1.64	-0.20
cameral sheets	211.28	1.055	0.22	4.11	-1.06	0.46
shell	1254.86	2.670	3.35	6.44	6.10	0
body chamber	13867.30	1.055	14.63	3.18	8.54	0

TABLE 6. Masses and positions of total X, Y and Z coordinates for model 3 (cameral sheets optional). Total displacement and position of centre of buoyancy is also indicated.

Complete model	Mass (g)	X coordinate (mm)	Y coordinate (mm)	Z coordinate (mm)
without cameral membranes	18.17	3.78	7.98	0
with cameral membranes	18.39	3.79	7.88	0.01
displacement	18.37	3.44	6.65	0

be positively buoyant in order to allow for the presence of cameral liquid in the youngest chambers of the phragmocone. As discussed in Ward (1987), as each new chamber is added to the phragmocone of *Nautilus*, it is initially filled with cameral liquid, which remains until the newly secreted septum is strong enough to withstand pressure at depth. Once the septum reaches about one half of its ultimate thickness, emptying of the chamber begins. In addition to this, the penultimate chamber still contains some liquid, which can be on the order of about one third of the chamber volume. In the current paper, models 2 and 3 both represent immature ammonites and thus, significant cameral liquid was probably present in the last two phragmocone chambers. However, when considering the total mass of the models relative to the mass of the displaced water, model 2 (DMAX = 300 mm) is 1.02 % negatively buoyant if cameral membranes are not included and 2.26 % negatively buoyant if cameral membranes are included (Table 4) whereas model 3 (DMAX = 54 mm) is 1.10 % positively buoyant if cameral membranes are not considered and 0.11 % negatively buoyant if cameral membranes are considered (Table 6). In both cases, the models are too heavy. This discrepancy may be due to inaccuracies in the densities used for individual components, diagenetic alteration of the original material that affected the measurements or human error. Alternatively, as in most studies of ammonoid hydrostatics, we considered the body chamber to be completely full of soft tissue, which may not be accurate (Kröger 2002). Finally, the indirect method used to ascertain the mature body chamber length as discussed above may have led to an overestimate in length. Juvenile Ammonitina generally have a longer body chamber than adult shells (Westermann 1971; Lehmann 1981) whereas in our models, the body chamber length was held constant at 259 degrees. Although model 2 does not represent a mature specimen, it does represent a specimen that is much larger than is represented in model 3, and it is possible that it would have had a shorter body chamber. This may explain the increased error in model 2 compared to model 3. Whatever the cause, these discrepancies in mass are not very large and do not have a significant effect on the results of our study.

Model 1 suggests a counterbalance mechanism may have been present, which allowed the animal to remain upright with its plane of bilateral symmetry vertical in the water column. When only the siphuncle and septum are considered, the moment created by the septum offsets about 295 % of the moment created by the siphuncle (Table 2). In this case, the model leans away from the direction of the siphuncle. When the optional cameral sheets are included in the model, the moment created by the septum offsets about 36 % of the moment created by the siphuncle and cameral sheets (Table 2). In this case, the model leans toward the siphuncle. In both cases, although the correction is not perfect, it does suggest a counterbalance may have been in effect.

In the large model of the complete ammonite (model 2), each component of the animal has a very different centre of mass (Table 3; Figure 11). However, the masses of the asymmetric components in the ammonite phragmocone are very low when compared to the mass of the entire animal. When cameral sheets are not considered, the siphuncle is less than 0.1 %, and the septa are about 1.4 % of the total mass of the animal (Tables 3-4). When cameral sheets are considered, the siphuncle is less than 0.1 %, the septa are about 1.4 % and the cameral sheets are approximately 1.2 % of the total mass of the animal (Tables 3-4). The offset of the centre of mass in the Z-plane (indicated by the final Z-coordinates in Table 4) is very small (about -0.01 mm if cameral membranes are not considered and approximately 0.02 mm if cameral membranes are considered). The size of these numbers is partially due to the correction discussed in model 1 where the position of the centroid of the siphuncle (and the centroid of the optional cameral sheets) is counterbalanced by the position of the centroid of the septa in the Z-plane (Table 2). Nevertheless, in terms of the whole model, removing the offset mass of the septa only changes the flotation angle by approximately 0.20 degrees. This figure is within our range of error and demonstrates that the effects of the asymmetries in the components of the phragmocone on flotation angle are virtually negligible at large shell diameters.

Although each component of the animal has a very different centre of mass in the small ammonite model (model 3; Table 5), the masses of the asymmetric components in the ammonite phragmocone are very low when compared to the mass of the entire animal, similar to the situation in the large model. When cameral sheets are not considered, the siphuncle is just over 0.1 %, and the septa are slightly over 0.9 % of the total mass of the animal (Tables 5-6). When cameral sheets are considered, the siphuncle is just over 0.1 %, the septa are just over 0.9 % and the cameral sheets are approximately 1.2 % of the total mass of the animal (Tables 5-6). The final Z-coordinates are very small at virtually 0 mm if cameral membranes are not considered and about 0.01 mm if cameral membranes are considered (Table 6). Once again, the size of these numbers is partially due to the correction discussed in model 1 where the position of the centroid of the siphuncle (and the centroid of the optional cameral sheets) is counterbalanced by the position of the centroids of the septa (Table 2). However, in terms of the whole model, removing the offset mass of the septa only changes the flotation angle by approximately 0.14 degrees. Similar to the large model, this figure is within our range of error and demonstrates that the affects of the asymmetries in the components of the phragmocone on flotation angle are virtually negligible at small shell diameters.

One potential issue that is not considered in models 2 and 3 is the possibility of asymmetries in the soft tissues of the body chamber. Hengsbach (e.g., 1979 and references therein) suggested that asymmetries in the suture line may be a consequence of asymmetries of the internal organs within the body chamber. If this were the case, it is possible that heavier soft body parts may have influenced the hydrostatics of the animal. Currently it is not possible to consider this directly in the model, as the specifics of the structure of the soft body of *B. columbiae* are unknown. However, it is possible to use an indirect approach to look for asymmetries. Checa et al. (2002) demonstrated that in cases where an epizoan infested one side of an ammonite, the whorl would shift in subsequent growth, to 'correct' for the permanently tilted ammonite and allow the aperture to grow upwards within the vertical plane. Over time, this gave rise to trochospiral coiling of the shell. Checa et al. (2002) suggested that ammonites contain morphogenetic instructions that constrain growth direction to the vertical plane. By analogy, if the mass of the soft body of the modeled *B. columbiae* were unevenly distributed in the living chamber, it would be expected that the shell would show some degree of trochospiral coiling. However, we examined over 500 complete or nearly complete specimens of *Badouxia*, which consistently showed asymmetry in their siphuncle and septa. No appreciable deviation from planispiral coiling was evident

(Longridge et al. 2006). This suggests that asymmetries within the body chamber of *B. columbiae* were not a significant factor.

Another consideration is how sensitive the models are to small changes of mass in the individual components. To test the sensitivity, we altered model 2 (including cameral sheets) in two different ways. Firstly, to consider the affects of a change in density, we altered the density of the septa and shell from 2.67 g/cm^3 to 2.62 g/cm^3 (the density of *Nautilus* shell as given in Reyment 1958 and Saunders and Shapiro 1986). This change altered the masses of the septa and shell by 0.75 g and 10.97 g, respectively, and had only a very small effect on the centre of mass of the animal, with a change of 0.06 mm in the X-plane, 0.04 mm in the Y-plane and no change in the Z-plane. Secondly, to consider the affects of a change in volume, we altered the length of the body chamber to 285 degrees. This alteration changed the volume of the body chamber by 67601.80 mm^3, increasing the mass of the animal by 71.32 g. This change altered the position of the centre of mass of the animal in the X-plane by 0.34 mm, in the Y-plane by 2.7 mm and had no effect in the Z-plane. Based on these analyses, the model seems reasonably robust to minor changes in the densities and volumes of individual components, particularly in the Z-plane.

SUMMARY AND CONCLUSIONS

The centroids of the internal components of the phragmocone including septa, siphuncle and possibly cameral sheets were offset from the centre in the Sinemurian ammonite, *B. columbiae*. When only these asymmetric components are considered in isolation, a counterbalance mechanism seems to be present. The mass of the offset siphuncle (with optional cameral sheets) is at least partially corrected by the mass of the septa, which is displaced in the opposite direction in the Z-plane. However, when the complete animal is considered at both large and small shell diameters, the individual components within the phragmocone are very small with respect to the mass of the entire animal and the effect of the offset components is virtually negligible. Thus, the existence of a weight-balancing mechanism seems unlikely. More probably, the asymmetry in the position of the siphuncle simply forced expansion of the suture line and associated septal folding on the opposite side. Although the displaced masses on either side of the plane of bilateral symmetry did counterbalance each other to some extent, their magnitude relative to the mass of the entire animal was inconsequential.

ACKNOWLEDGEMENTS

This study was supported by an NSERC grant to PLS. This paper has been significantly improved by the helpful comments of B. Kröger and two anonymous reviewers. We thank S. Calisal for the use of his laboratory, S. Wilson for her help with x-ray diffraction as well as N. Longridge, H. Garrow and M. Raudsepp for technical discussions on various components used in model construction.

REFERENCES

Canavari, M. 1882. Beiträge zur Fauna des unteren Lias von Spezia, *Palaeontographica*, 29:125-192, pls. 15-21.

Checa, A.G., Okamoto, T. and Keupp, H. 2002. Abnormalities as natural experiments: a morphogenetic model for coiling regulation in planispiral ammonites. *Paleobiology*, 28:127-138.

Diener, C. 1912. Lebensweise und Verbreitung der Ammoniten. *Neues Jahrbuch Mineralogie, Geologie, und Paläeontologie, Jahrgang*, 2:67-89.

Erben, H.K. and Reid, R.E. 1971. Ultrastructure of shell, origin of conellae and siphuncular membranes in an ammonite. *Biomineralisation*, 3:22-31.

Frebold, H. 1967. Hettangian ammonite faunas of the Taseko Lakes map area, British Columbia. *Geological Survey of Canada Bulletin*, 158:1-35, 9 pls.

Grandjean, F. 1910. Le siphon des ammonites et des belemnites. *Société Géologique de France Bulletin*, 10:496-519.

Guex, J. 2001. Environmental stress and atavism in ammonoid evolution. *Eclogae Geologicae Helvetiae*, 94:321-328.

Guex, J. 2006. Reinitialization of evolutionary clocks during sublethal environmental stress in some invertebrates. *Earth and Planetary Science Letters*, 242:240-253.

Hengsbach, R. 1979. Zur kenntnis der asymmetrie der ammoniten-lobenlinie. *Zoologische Beiträge*, 25:107-162.

Hengsbach, R. 1986a. Über *Arnioceras falcaries* (Quenstedt) und einige verwandte Arten aus Mitteldeutschland (Ammonoidea; Lias). *Senckenbergiana Lethaia*, 67:151-170.

Hengsbach, R. 1986b. Ontogenetisches Auftreten und Entwicklung der Sutur-Asymmetrie bei einigen Psiloceratacea (Ammonoidea; Jura). *Senckenbergiana Lethaia*, 67:323-330.

Hengsbach, R. 1991. Studien zur Paläopathologie der Invertebraten III: Parasitismus bei Ammoniten. *Paläontologische Zeitschrift*, 65:127-139.

Hengsbach, R. 1996. Ammonoid pathology, p. 581-605. In Landman, N., Tanabe, K. and Davis, R.A. (eds.), *Ammonoid Paleobiology, Volume 13 of Topics in Geobiology*. Plenum Press, New York.

Hewitt, R.A. and Westermann, G.E.G. 1996. Post-mortem behaviour of Early Paleozoic nautiloids and paleobathymetry. *Paläontologische Zeitschrift*, 70:405-424.

Hoffman, A.A. and Parsons, P.A. 1991. *Evolutionary Genetics and Environmental Stress*. Oxford Science Publications, Oxford.

Hölder, H. 1956. Über Anomalien an jurassischen Ammoniten. *Paläontologische Zeitschrift*, 30:95-107.

Kröger, B. 2002. On the efficiency of the buoyancy apparatus in ammonoids: evidences from sublethal shell injuries. *Lethaia*, 35:61-70.

Kulicki, C. 1996. Ammonoid shell microstructure, p. 65-96. In Landman, N., Tanabe, K. and Davis, R.A. (eds.), *Ammonoid Paleobiology, Volume 13 of Topics in Geobiology*. Plenum Press, New York.

Lehmann, U. 1981. *The Ammonites: Their Life and Their World*. Cambridge University Press, Cambridge.

Liu, M. and Yund, R.A. 1993. Transformation kinetics of polycrystalline aragonite to calcite: new experimental data, modelling, and implications. *Contributions to Mineralogy and Petrology*, 114:465-478.

Longridge, L.M., Smith, P.L. and Tipper, H.W. 2006. The Early Jurassic ammonite *Badouxia* from British Columbia, Canada. *Palaeontology*, 49:795-816.

Raup, D.M. 1967. Geometric analysis of shell coiling: coiling in ammonoids. *Journal of Paleontology*, 41:43-65.

Reyment, R.A. 1958. Some factors in the distribution of fossil cephalopods. *Stockholm Contributions in Geology*, 1:97-184.

Saunders, W.B. and Shapiro, E.A. 1986. Calculation and simulation of ammonoid hydrostatics. *Paleobiology*, 12:64-79.

Smith, P.L. 1986. The implications of data base management systems to paleontology: A discussion of Jurassic ammonoid data. *Journal of Paleontology*, 60:327-340.

Spath, L.F. 1919. Notes on Ammonites III. *Geological Magazine*, 56:115-122.

Swinnerton, H.H. and Trueman, A.E. 1917. The morphology and development of the ammonite septum. *Quarterly Journal of the Geological Society of London*, 73:26-58.

Tanabe, K., Kulicki, C. and Landman, N.H. 2005. Precursory siphuncular membranes in the body chamber of *Phyllopachyceras* and comparisons with other ammonoids. *Acta Palaeontologica Polonica*, 50:9-18.

Tanabe, K., Mapes, R.H., Sasaki, T. and Landman, N.H. 2000. Soft-part anatomy of the siphuncle in Permian prolecanitid ammonoids. *Lethaia*, 33:83-91.

Trueman, A.E. 1941. The ammonite body-chamber, with special reference to the buoyancy and mode of life of the living ammonite. *Quaternary Journal of the Geological Society of London*, 96:339-383.

Ward, P.D. 1987. *The Natural History of* Nautilus. Allen and Unwin Press, London.

Weitschat, W. and Bandel, K. 1991. Organic components in phragmocones of Boreal Triassic ammonoids: Implications for ammonoid biology. *Paläontologische Zeitschrift,* 65:269-303.

Westermann, G.E.G. 1971. Form, structure and function of shell and siphuncle in coiled Mesozoic ammonoids. *Life Sciences Contributions of the Royal Ontario Museum*, 78:1-39.

Westermann, G.E.G. 1992. Formation and function of suspended organic cameral sheets in Triassic ammonoids – discussion. *Paläontologische Zeitschrift*, 66:437-441.

Westermann, G.E.G. 1996. Ammonoid life and habitat, p. 607-706. In Landman, N., Tanabe, K. and Davis, R.A. (eds.), *Ammonoid Paleobiology, Volume 13 of Topics in Geobiology*. Plenum Press, New York.

Westermann, G.E.G. 1998. Life habits of Nautiloids, p. 263-298. In Savazzi, E. (ed.), *Functional morphology of the invertebrate skeleton*. John Wiley and Sons, New York.